Recovery From Overt Type 1 Diabetes Ensues When Immune Tolerance and β-Cell Formation Are Coupled With Regeneration of Endothelial Cells in the Pancreatic Islets

Xiaoxiao Wan,[1] F. Betul Guloglu,[1] Amie M. VanMorlan,[2] Linda M. Rowland,[1] Sarah Zaghouani,[1] Jason A. Cascio,[1] Mermagya Dhakal,[1] Christine M. Hoeman,[1] and Habib Zaghouani[1,2,3]

Immune modulation of pancreatic inflammation induces recovery from type 1 diabetes (T1D), but remission was not durable, perhaps because of an inability to sustain the formation and function of new pancreatic β-cells. We have previously shown that Ig-GAD2, carrying GAD 206–220 peptide, induced in hyperglycemic mice immune modulation that was able to control pancreatic inflammation, stimulate β-cell regeneration, and prevent T1D progression. Herein, we show that the same Ig-GAD2 regimen given to mice with overt T1D was unable to reverse the course of disease despite eradication of Th1 and Th17 cells from the pancreas. However, the regimen was able to sustain recovery from T1D when Ig-GAD2 was accompanied with transfer of bone marrow (BM) cells from healthy donors. Interestingly, alongside immune modulation, there was concomitant formation of new β-cells and endothelial cells (ECs) in the pancreas. The new β-cells were of host origin while the donor BM cells gave rise to the ECs. Moreover, transfer of purified BM endothelial progenitors instead of whole BM cells sustained both β-cell and EC formation and reversal of diabetes. Thus, overcoming T1D requires both immune modulation and repair of the islet vascular niche to preserve newly formed β-cells. *Diabetes* 62:2879–2889, 2013

Type 1 diabetes (T1D) is a chronic disease in which the insulin-producing β-cells of the pancreatic islets are destroyed by inflammatory T lymphocytes of the immune system (1,2). Broad-based T-cell–targeted therapies, such as anti-CD3 monoclonal antibodies, were able to reverse established overt T1D in the NOD mouse (3). In humans, however, although the regimen preserved C-peptide responses, disease rebounded even when the antibody was used in a non-Fc receptor binding form (4,5). Nonspecific activation of T cells was perhaps responsible for the return of inflammation and β-cell dysfunction. Thus, we reasoned that antigen-specific therapy that targets mostly self-reactive T cells with minimal interference with other specificities

would be effective against the disease. In a previous study, we expressed the suppressive GAD 206–220 peptide (6) on an Ig molecule, and the resulting Ig-GAD2 was able to prevent disease progression in NOD mice that were diagnosed with insulitis (7). Moreover, Ig-GAD2 was effective against the disease even when the treatment was applied at the hyperglycemic stage where the blood glucose level (BGL) began to rise between 160 and 250 mg/dL (7). Interestingly, the animals restored normoglycemia (≤140 mg/dL), which was long-lasting due to effective immune modulation of pancreatic inflammation and, most importantly, stimulation of β-cell division and generation of healthy islets (7). These observations prompted us to test Ig-GAD2 for treatment of overt T1D (BGL ≥300 mg/dL), which would be more relevant to human circumstances. However, the regimen failed to sustain β-cell regeneration and overcome overt T1D despite induction of immune modulation and eradication of pancreatic infiltration. Given that β-cell mass is diminished at the diabetic stage and that bone marrow (BM) transplantation sustained regeneration of endogenous β-cells in streptozotocin (STZ) models of diabetes (8,9), we sought to determine whether enrichment with donor BM cells during treatment with Ig-GAD2 would restore β-cell regeneration and counter overt diabetes. This was indeed feasible, as β-cell formation ensued and the mice recovered from overt T1D. Surprisingly, however, there was engraftment of endothelial cells (ECs) and these were of donor BM origin, whereas the newly formed β-cells were derived from host cells. Moreover, substitution of whole BM with endothelial progenitor cells (EPCs) during treatment with Ig-GAD2 allowed for restoration of both ECs and β-cells and recovery from overt T1D. These findings indicate that recovery from overt T1D necessitates repair of both β-cell mass and the islet endothelial niche.

RESEARCH DESIGN AND METHODS

Mice. NOD and NOD.GFP mice expressing the green fluorescence protein (GFP) under the β-actin promoter were previously described (10) and were maintained in the Animal Facility at the Medical Sciences Building under barrier conditions. All animals were treated in accordance with the guidelines of the University of Missouri Animal Care and Use Committee.

Treatment with Ig-GAD2 and donor BM. Mice began BGL monitoring at 10 weeks of age, and those displaying ≥300 mg/dL for two consecutive weeks (considered overtly diabetic) were enrolled in the treatment regimen. The mice were first given two sustained-release insulin implants (LinShin, Toronto, ON, Canada) inserted subcutaneously in the abdomen to temporarily maintain normoglycemia for 2–3 weeks. The mice were then given 300 μg Ig-GAD2 i.p. three times weekly for 5 weeks and then once a week for another 5 weeks. Donor BM cells were isolated from the femur and tibia of healthy (non-diabetic) NOD mice, and 10×10^6 cells were transferred intravenously weekly

on weeks 2, 3, and 4 postdiagnosis. The mice were monitored for BGL until day 120. In some experiments (Fig. 1A), treatment with Ig-GAD2 alone was applied to hyperglycemic mice when BGLs were 160–250 mg/dL for two consecutive measurements 3 days apart.

Treatment with Ig-GAD2 and donor EPCs. This regimen was similar to treatment with Ig-GAD2 and donor BM except that EPCs substituted for whole BM cells. FLK-1$^+$ EPCs were given at 5×10^4 per injection whereas FLK-1$^-$ EPCs were given at 3×10^6 cells per injection.

Purification of EPCs. BM cells were harvested from healthy or diabetic (sick) mice and depleted of lineage$^+$ (Lin$^+$) cells using the lineage cell depletion kit according to the manufacturer's instruction (Miltenyi Biotec). The Lin$^-$ cells were stained with anti–c-Kit and anti–FLK-1 antibodies as well as 7-amino-actinomycin D (7-AAD) and sorted into c-Kit$^+$7-AAD$^-$FLK-1$^+$ or c-Kit$^+$7-AAD$^-$FLK-1$^-$ cells.

Cell surface staining. For detection of platelet endothelial cell adhesion molecule (PECAM)1, FLK-1, c-Kit, and CD45, the cells were stained with marker-specific antibodies, including phycoerythrin (PE)-cy7–conjugated anti-PECAM1 (390), allophycocyanin (APC)-conjugated anti-FLK1 (Avas12a1) (both from eBiosciences), PE-cy5.5–conjugated anti–c-Kit (2B8), and APC-cy7–conjugated anti-CD45 (2D1) (both from BD Pharmingen) antibodies. For detection of apoptotic cells, cells were stained with 7-AAD (EMD Biosciences).

Intracellular staining. For detection of intracellular interferon-γ (IFN-γ), interleukin-10 (IL-10), and IL-17 in CD4$^+$ T cells, the cultures were stimulated with phorbol myristic acid (PMA) (50 ng/mL) and ionomycin (500 ng/mL) for 4 h in the presence of brefeldin A (10 μg/mL) and then stained with peridinin-chlorophyll-protein (PerCP)-cy5.5–conjugated anti-CD4 (RM4-5), PE-conjugated anti-Vβ8.1/8.2 (MR5-2), and fluorescein isothiocyanate (FITC)–conjugated anti-CD8 (RPA-T8) antibodies (all from BD Pharmingen). Subsequently, the cells were fixed with 2% formaldehyde, permeabilized with 0.2% saponin, and stained with PE-cy7–conjugated anti–IFN-γ (XMG1.2), APC-conjugated anti–IL-10 (JES5–16E3), or APC-conjugated anti–IL-17 (eBio17B7) antibody (all from eBiosciences).
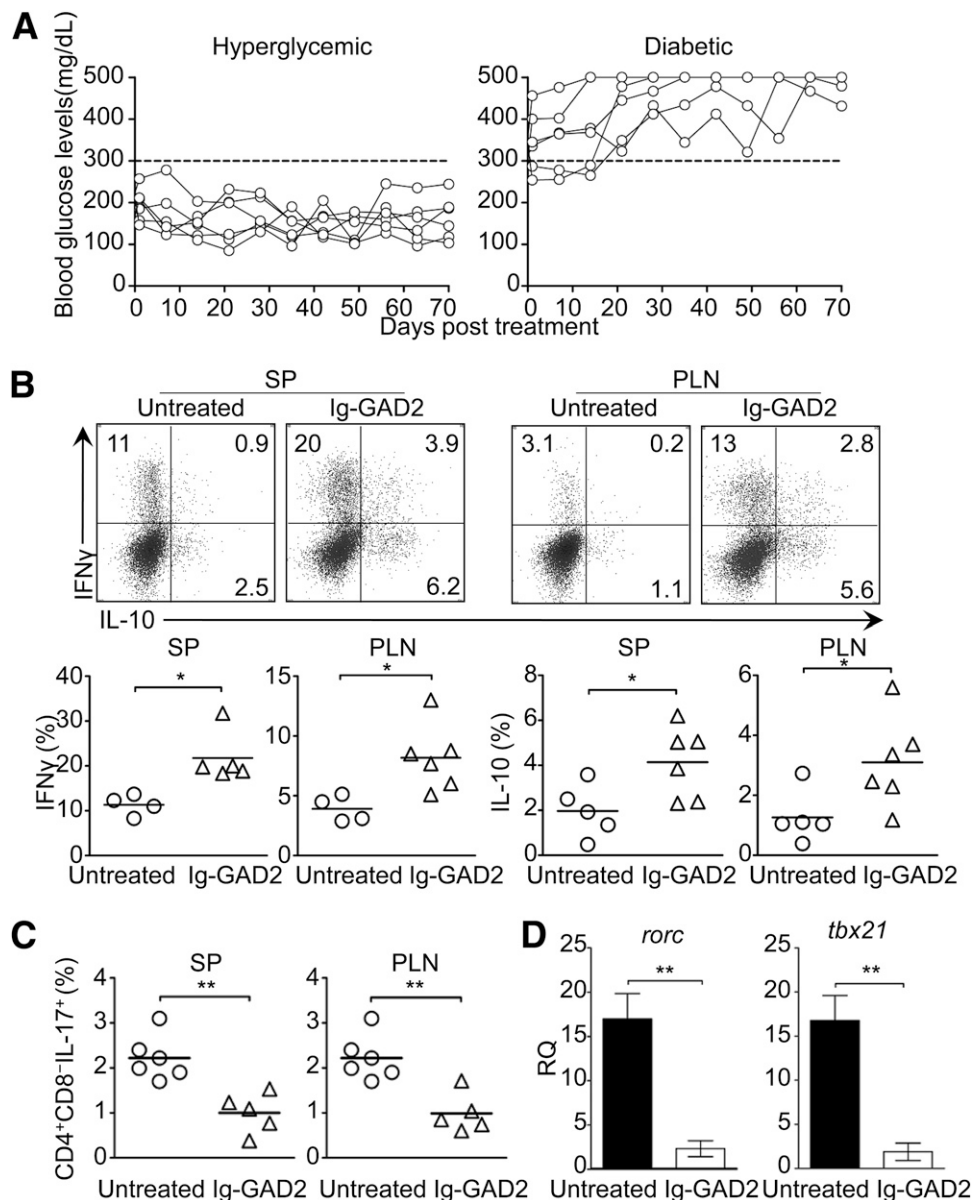

FIG. 1. Ig-GAD2 treatment could not overcome overt T1D despite induction of immune tolerance. *A*: Hyperglycemic (BGL = 160–250 mg/dL) and diabetic (BGL ≥300 mg/dL) NOD mice (six per group) were given Ig-GAD2, and their BGLs were monitored for a period of 70 days. *B* and *C*: The mice of the diabetic group were killed on day 70 and the SP and PLN cells were harvested, stimulated with PMA and ionomycin, and stained for surface CD4, CD8, and Vβ8.1/8.2 as well as intracellular IFN-γ, IL-10, and IL-17. A group of mice killed upon diagnosis of diabetes (untreated) was used as control. *B*: Representative FACS plots (*top*) and individual mice (*bottom*) depicting CD4$^+$CD8$^-$Vβ8.1/8.2$^+$ cells producing IFN-γ and IL-10. *C*: The frequency of CD4$^+$CD8$^-$IL-17$^+$ cells. *D*: The RQ of mRNA expression for RORγt (*rorc*) and T-bet (*tbx21*) in the pancreatic islets of untreated and Ig-GAD2–treated mice. Each bar represents mean ± SEM of three to six mice. *$P < 0.05$; **$P < 0.01$.

Flow cytometry analyses. The samples were read using a Beckman Coulter CyAn ADP, and data were analyzed using Summit V4.3 (Dako). Cell sorting (>98% purity) was performed using a Beckman Coulter MoFlo XDP sorter.

Sample preparation for histologic analyses. Pancreata were frozen in tissue-freezing medium (Triangle Biomedical Sciences), and nonserial 8-µm-thick sections were cut 150 µm apart to avoid overcounting of the labeled cells. The sections were fixed in 4% formaldehyde for 10 min before histological procedures. For detection of enhanced GFP expression in tissues, pancreata were fixed in 4% formaldehyde for 4 h at 4°C and immersed in 30% sucrose overnight before freezing. For analysis of insulitis, hematoxylin-eosin staining was used as previously described (7). Each experiment used three to six sections per pancreas.

Immunohistochemistry. For detection of β-cells, pancreatic sections were incubated with horseradish peroxidase–conjugated anti-insulin affibody molecule (1:200; Abcam) at room temperature (RT) for 45 min, and the insulin⁺ cells were identified by incubating the slides with DAB chromogen and substrate (ScyTek) for 5 min. The cell nuclei were counterstained with hematoxylin.

Immunofluorescence. Pancreatic sections were treated with a PBS solution containing 1% BSA, 10% goat or donkey serum, and 0.2% Triton X-100 at RT for 1 h. The sections were then incubated overnight at 4°C with primary antibodies, including rabbit anti-insulin (1:200; Santa Cruz Biotechnology), guinea pig anti-insulin (1:300; Abcam), rabbit anti-PECAM1 (1:100; Abcam), goat anti-PECAM1 (1:100; Santa Cruz Biotechnology), rabbit anti–ki-67 (1:300; Abcam), and goat anti-VEGF (1:200; Santa Cruz Biotechnology). The slides were washed with three changes of 0.02% Triton X-100 in PBS and then stained for 1 h at RT with the corresponding secondary antibodies, including Texas Red–conjugated goat anti-rabbit IgG (1:200), FITC-conjugated goat anti–guinea pig IgG (1:200), FITC-conjugated donkey anti-goat IgG (1:200) (all from Santa Cruz Biotechnology), DyLight 405–conjugated donkey anti-rabbit IgG (1:200), and DyLight 549–conjugated donkey anti-goat IgG (1:300) (all from Jackson ImmunoResearch). In some experiments, the cell nuclei were counterstained with DAPI (Santa Cruz Biotechnology). The images were visualized and acquired with a Zeiss fluorescence microscope or an Olympus DSU confocal microscope. The number of β-cells, islets, and ECs was scored with a computer-assisted Image Pro Plus program (Media Cybernetics, Silver Spring, MD).

Measurement of β-cell mass. Pancreata were weighed and used to prepare frozen sections. The slides were stained for insulin by immunohistochemistry, and β-cell mass was determined by point-counting morphometry as well as pixel-based technology as previously described (11). Despite the fact that β-cell mass quantification was validated by both technologies, Fig. 3 incorporates only data calculated by pixel-based technology. In brief, cross-sectional areas of insulin⁺ cells were measured at 150-µm intervals and normalized to total pancreatic area using the Image-Pro Plus program. β-Cell mass is expressed in milligrams after normalization to total pancreatic mass. For each pancreas, 30 sections were cut and used for different experiments. For determination of β-cell mass, six nonserial sections (5th, 10th, 15th, 20th, 25th, and 30th) spanning both proximal and distal areas of the pancreas were used.

Laser capture microdissection. Pancreatic sections were stained with insulin or PECAM1 and thoroughly dehydrated with the Arcturus dehydration component. The insulin⁺ or PECAM1⁺ cells were dissected with the CapSure HS LCM caps and the Autopix 100 laser capture microdissection system by following the manufacturer's instructions. For each individual mouse, cells were dissected from 3–10 nonserial sections. Genomic DNA was extracted from the dissected cells using the PicoPure DNA extraction kit. All the reagents are from Applied Biosystems.

Detection of Y chromosome by PCR. Detection of Y chromosome and β-actin was performed using a 20-ng DNA template and Maxima qPCR master mix (Fermentas). The sequences of the primers are listed in Supplementary Table 1.

Quantitative PCR analysis. Total RNA was extracted from pancreatic islets using the TRI RNA isolation reagent (Sigma-Aldrich). Quantitative PCR was performed using the Power SYBR Green kit and the StepOnePlus instrument (all from Applied Biosystems). The relative quantity (RQ) was calculated based on the ΔΔCT after normalization with the internal control 18S ribosome RNA expression. The sequences of the primers for T-cell transcription factors and genes involved in EC function are listed in Supplementary Table 1.

Statistical analyses. P values associated with all pairwise comparisons were calculated based on Student t test for independent groups. Error bars were defined using SEM.

RESULTS

Ig-GAD2–driven immune modulation is not sufficient to overcome overt T1D. In a prior study, we showed that Ig-GAD2 can restore normoglycemia in NOD mice that begin to display a rise in BGL (160–250 mg/dL) and are referred to as hyperglycemic (7). The immune mechanisms underlying protection against the disease manifest in the form of reduced cell infiltration in the pancreas associated with eradication of both Th1 and Th17 cells (7). However, although no Th17 cells were observed in the pancreatic lymph nodes (PLN) or the spleen (SP), there were residual Th1 cells retained in the latter organ, but these were nonpathogenic (7). We therefore tested the regimen against overt T1D (BGL ≥300 mg/dL), which would be more relevant to human circumstances. To our surprise, however, there was no restoration of normoglycemia in overtly diabetic mice, despite the fact that Ig-GAD2–driven immune modulation was similar to that in the hyperglycemic mice that recovered from disease (Fig. 1). Indeed, although all hyperglycemic mice displayed a reduction in BGL, none of the diabetic animals recovered from diabetes (Fig. 1A). More intriguing, the sick animals displayed eradication of Th17 cells and retention of Th1 cells in the SP (Fig. 1B–D). In fact, the Ig-GAD2–treated diabetic mice had increased frequency of CD4⁺CD8⁻Vβ8.1/8.2⁺ T cells producing IFN-γ and/or IL-10 (Fig. 1B) but diminished Th17 cells in the SP and PLN relative to untreated sick animals (Fig. 1C). Moreover, there were reduced Th1 or Th17 cells in the pancreas because the mRNA for their signature transcription factors, T-bet and RORγt, respectively, were significantly diminished (Fig. 1D). Overall, Ig-GAD2–driven immune modulation is not sufficient to restore normoglycemia in overtly diabetic mice.

Transfer of BM cells alongside Ig-GAD2 treatment overcomes overt T1D. It has previously been shown that adult β-cells are formed mainly by self-duplication (12). Given the fact that in diabetic mice, most of the β-cells are destroyed and self-duplication would be minimal, we reasoned that Ig-GAD2 treatment would overcome overt T1D if β-cell regeneration is restored. Since BM transplantation has been shown to support regeneration of endogenous β-cells and restore normoglycemia in STZ-induced diabetes (8,9), it is logical to envision that enrichment with BM cells during suppression of inflammation with Ig-GAD2 would counter overt diabetes. To test this premise, we combined BM cell transfer from healthy donors with a 70-day Ig-GAD2 treatment (Fig. 2A) and assessed for reduction in BGL. Figure 2B shows that the majority of the mice given both Ig-GAD2 and BM transfer (Ig-GAD2+BM) returned to BGL <300 mg/dL whether the BM was from male or female donors (Fig. 2B). Despite the fact that some of the mice restored normoglycemia (BGL <140 mg/dL) whereas others reduced their BGL only to hyperglycemic levels (160–250 mg/dL), they were all used for mechanistic analyses without distinction. Furthermore, the treatment ablated insulin resistance associated with the onset of diabetes (Supplementary Fig. 1) as was observed in models of non–antigen-specific regimens (13,14). No protection was observed in mice given Ig-GAD2 or BM alone (Fig. 2B). The enrichment with BM cells sustained protection against disease without impacting Ig-GAD2–mediated immune modulation. Indeed, the diabetic mice treated with the combination (Ig-GAD2+BM) regimen, like those receiving Ig-GAD2 alone, had increased frequency of CD4⁺CD8⁻Vβ8.1/8.2⁺ T cells producing IFN-γ and/or IL-10 (Fig. 2C) but diminished Th17 cells in the SP and PLN (Fig. 2D). In contrast, mice receiving BM alone that remained sick had no increase in IFN-γ– and IL-10–producing cells or decrease in Th17 cells (Fig. 2C and D). Moreover, in the pancreas of Ig-GAD2+BM groups, the mRNA for T-bet and
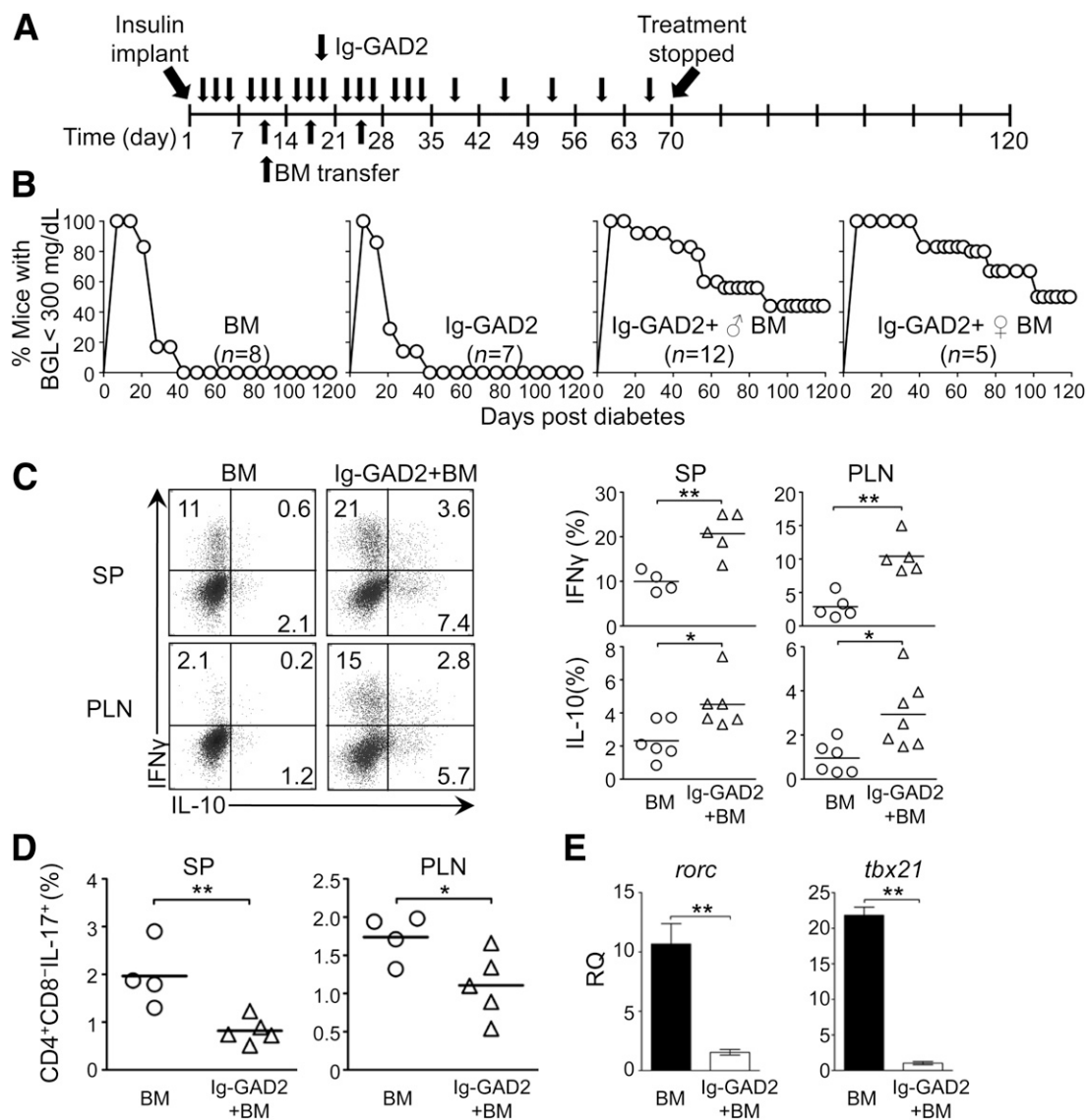
FIG. 2. Healthy donor BM cells transferred during immune modulation restore normoglycemia in diabetic mice. *A*: Schematic representation of the treatment regimen in which diabetic mice received two insulin pellet implants on day 1 of the regimen and Ig-GAD2 and BM transfer as indicated. *B*: Percent of mice with BGL <300 mg/dL from groups receiving BM transfer alone (BM), Ig-GAD2 alone (Ig-GAD2), or Ig-GAD2 plus male or female BM. The *n* indicates the number of mice. *C* and *D*: SP and PLN cells of the mice receiving BM or Ig-GAD2+BM were harvested on day 70, stimulated with PMA and ionomycin, and analyzed for cytokine production. *C*: Representative FACS plots (*left*) and individual mice (*right*) depicting CD4$^+$CD8$^-$Vβ8.1/8.2$^+$ cells producing IFN-γ and IL-10. *D*: Frequency of IL-17–producing CD4$^+$CD8$^-$ cells. *E*: The RQ of mRNA expression for RORγt (*rorc*) and T-bet (*tbx21*) in the pancreatic islets of mice receiving BM or Ig-GAD2+BM. Each bar represents mean ± SEM of four to eight mice. *$P < 0.05$; **$P < 0.01$.

RORγt was significantly diminished relative to animals receiving BM alone (Fig. 2*E*), indicating that both Th1 and Th17 cells were minimal in this site. Overall, addition of BM transfer to the Ig-GAD2 regimen sustained protection against diabetes without impacting immune modulation.

BM transfer synergizes with Ig-GAD2 to drive formation of healthy islets. Since Ig-GAD2+BM but not Ig-GAD2 alone reduced BGL, it is possible that addition of BM transfer sustained regeneration of β-cells that were able to thrive under minimal inflammation curtailed by Ig-GAD2. To test these premises, the mice treated with Ig-GAD2+BM that displayed consistent return to BGL <300 mg/dL compared with those that received Ig-GAD2 or BM alone (Fig. 3*A*) were examined for reduction in pancreatic infiltration and formation of healthy islets. The results show that the mice that received Ig-GAD2+BM had islets that

were mostly free of insulitis or islets that had minimal infiltration in the form of peri-insulitis (Fig. 3*B* and *C*). Again, the mice that received Ig-GAD2 alone that were unable to recover from diabetes had islets with no or peri-insulitis, indicative of effective immune modulation. In contrast, the animals that received BM alone had mostly severe insulitis, indicating that the BM transfer without Ig-GAD2 does not directly modulate pancreatic inflammation (Fig. 3*B* and *C*). Moreover, whereas the mice treated with Ig-GAD2+BM had structured islets with abundant insulin-positive cells, those given Ig-GAD2 or BM alone had less islets with fewer β-cells like untreated, recently diagnosed diabetic mice (Fig. 3*D*). Compiled results indicate a significant increase in the number of insulin-producing β-cells, the number of islets with >10 insulin-positive cells, and the mass of β-cells in Ig-GAD2+BM–treated mice that was not evident
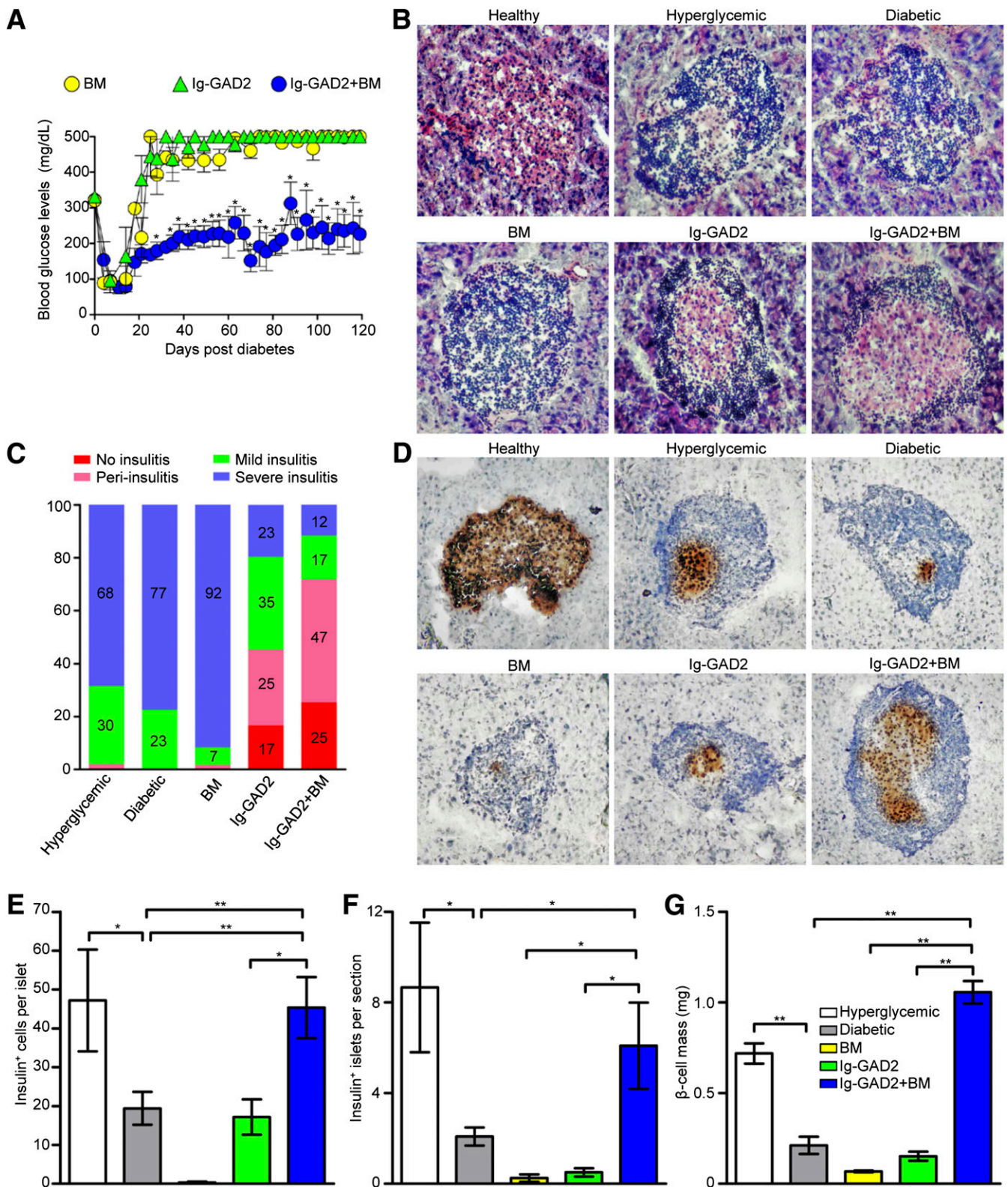
FIG. 3. Mice receiving BM transfer during treatment with Ig-GAD2 display increased insulin-producing pancreatic β-cells. *A*: BGLs in mice grafted with insulin pellets and given BM (*n* = 8), Ig-GAD2 (*n* = 7), or Ig-GAD2+BM (*n* = 17). *B*: Representative hematoxylin-eosin staining (100×) of pancreatic sections from mice recipient of BM, Ig-GAD2, or Ig-GAD2+BM (killed on day 70) (*n* = 6 per group). Unmanipulated 4- to 6-week-old healthy (BGL ≤140 mg/dL), hyperglycemic (BGL = 160–250 mg/dL), and recent-onset diabetic (BGL ≥300 mg/dL) mice are included as control. *C*: Islet infiltration severity scores of the indicated groups. *D*: Representative immunohistochemistry staining (100×) for insulin (brown) with nuclei counterstained with hematoxylin-eosin (blue). *E*: Quantification of insulin$^+$ cells per islet. *F*: Number of islets that contain >10 insulin$^+$ cells. *G*: Mass of β-cells. Results in *E–G* are based on the analysis of three to six nonserial sections per pancreas for six mice in each group. Specifically, at least 60 islets were counted for each of the new-onset diabetic, BM-treated, or Ig-GAD2–treated groups of mice. For the hyperglycemic and Ig-GAD2+BM–treated groups, at least 300 islets were counted per group. Error bars, mean ± SEM. *$P < 0.05$; **$P < 0.01$.

in animals recipient of Ig-GAD2 or BM alone (Fig. 3E–G). Since many islets in new-onset diabetic NOD mice have no insulin⁺ (degranulated) cells (15) and our detection quantified only those with insulin⁺ cells, it is possible that previously degranulated β-cells regained insulin-producing function in Ig-GAD2+BM–treated mice. Moreover, previous findings (7) and results below showing evidence of significant β-cell division suggest a role for β-cell regeneration in the increase of insulin-producing β-cells and healthy islets. Thus, the enrichment with BM cells synergized with Ig-GAD2–driven immune modulation to sustain an increase in the number of β-cells that were able to thrive and maintain the reduction in BGL.

Mice receiving BM transfer and Ig-GAD2 treatment display increased EC numbers in the pancreatic islets. The observation that BM transfer alongside Ig-GAD2 treatment sustains formation of healthy islets raises the question as to whether the newly formed β-cells originate from the donor BM cells. To test this premise, we used NOD.GFP mice (10) as a source of BM during treatment with Ig-GAD2 and assessed the insulin-producing β-cells for GFP expression. The results show that there was no GFP/insulin colocalization at any time point during Ig-GAD2+BM treatment (Supplementary Fig. 2, *left*). Furthermore, the GFP⁺ cells, which were abundant in the diabetes-free mice, were minimal in those receiving the same regimen but remaining diabetic (Supplementary Fig. 2, *right*). Thus, the BM transfer did not appear to serve as a source of insulin-producing β-cells but yielded engraftment of GFP⁺ cells in the islets of the recovering mice. Therefore, the β-cells did not originate from the donor cells as was observed in other models (8,9,16,17). The question then is whether the GFP⁺ engraftment represents cells that could not be provided by the host's BM but are

required for maintenance of endogenous β-cells. Given that the islets are highly vascularized with endothelial networks essential for optimal β-cell function (18–23), and that the number of functional ECs is compromised in diabetic mice (24–28), it is logical to envision that the donor GFP⁺ cells represent ECs. The results showing a significant decrease in the frequency of both circulating and intraislet PECAM1⁺ ECs in diabetic versus healthy mice (Fig. 4) support this postulate. Indeed, there was a dramatic decrease in the frequency of peripheral blood ECs as the mice progressed toward overt diabetes (Fig. 4A and B). Similarly, the frequency of ECs in the pancreatic islets diminished as the mice became diabetic, a phenomenon that correlates with the loss of β-cells (Fig. 4C and D). This indicates that the frequency of ECs is diminished both in the peripheral blood and in the pancreas in diabetic mice. Interestingly, the mice receiving Ig-GAD2+BM but not those given Ig-GAD2 or BM alone had restored PECAM1⁺ ECs in the islets (Fig. 5A). Moreover, when the expression of genes encoding VE-cadherin (*cdh5*), angiopoietin receptor (*tie1*), and vascular endothelial growth factor (VEGF) receptor 1 (*flt1*), which represent functional markers for ECs, was analyzed, there was a significant mRNA increase for these genes in the mice receiving Ig-GAD2+BM relative to untreated diabetic animals (Fig. 5B). Those given Ig-GAD2 or BM alone did not display a similar increase in the expression of the genes (Fig. 5B). The increase in ECs likely fosters angiogenesis for better islet vascularization and thriving of β-cells. In fact, there was a strong upregulation of genes encoding angiogenic factors, including VEGFa (*vegfa*), angiopoietin 1 (*angpt1*), and angiopoietin 2 (*angpt2*), in the pancreas of diabetes-free mice treated with Ig-GAD2+BM (Supplementary Fig. 3A). Furthermore, the newly formed β-cells produced VEGFa (Supplementary
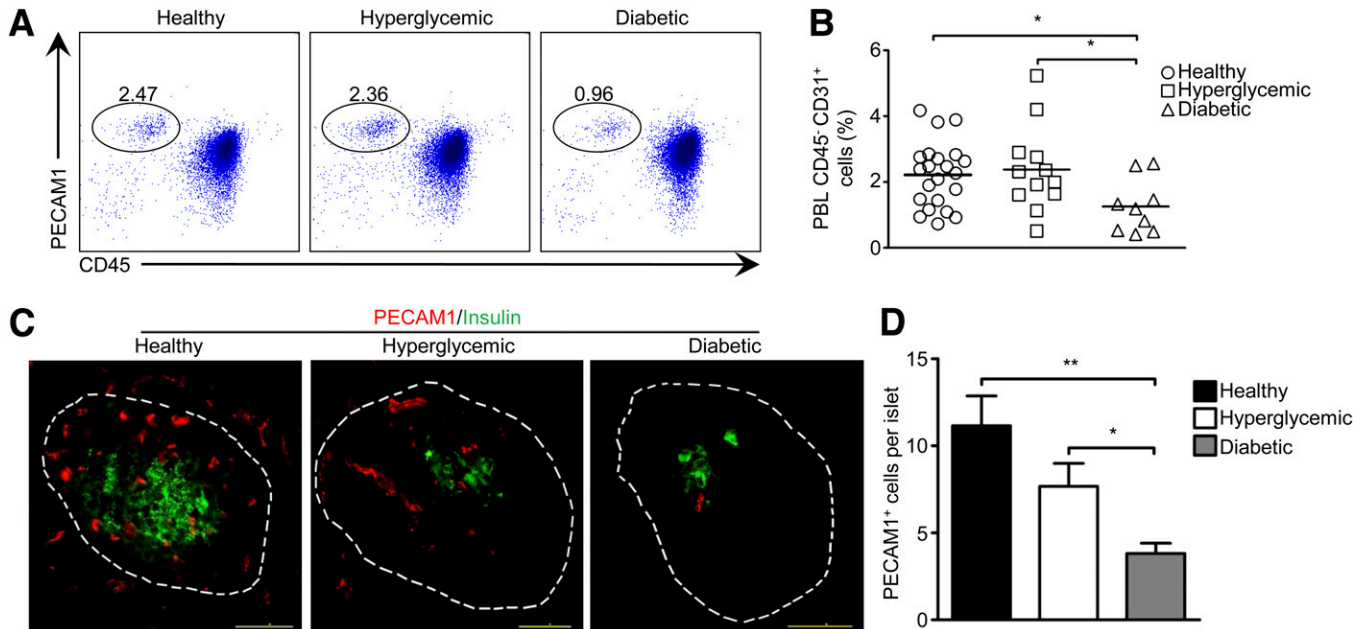

FIG. 4. Decline of blood and pancreatic ECs during progression to diabetes. *A* and *B*: Peripheral blood cells from unmanipulated 4- to 6-week-old healthy (*n* = 22), 8- to 14-week-old hyperglycemic (*n* = 12), and 15- to 30-week-old diabetic (*n* = 9) mice were stained with anti-CD45, anti-PECAM1, and 7-AAD, and PECAM1 expression was analyzed on 7-AAD⁻CD45⁻ gated cells. *A*: Representative FACS plots. *B*: Results of individually tested mice in each group. *C* and *D*: Nonserial pancreatic sections from the same groups of mice were stained for insulin (green) and PECAM1 (red) and analyzed by immunofluorescence microscopy. *C*: A representative staining within the boundary of an islet area. Scale bars, 50 μm. *D*: The number of PECAM1⁺ cells per islet. This was determined by nuclear counterstaining with DAPI. At least 40 islets from three to six nonserial sections per mouse were analyzed. Each bar represents mean ± SEM of five mice per group. *P < 0.05; **P < 0.01.
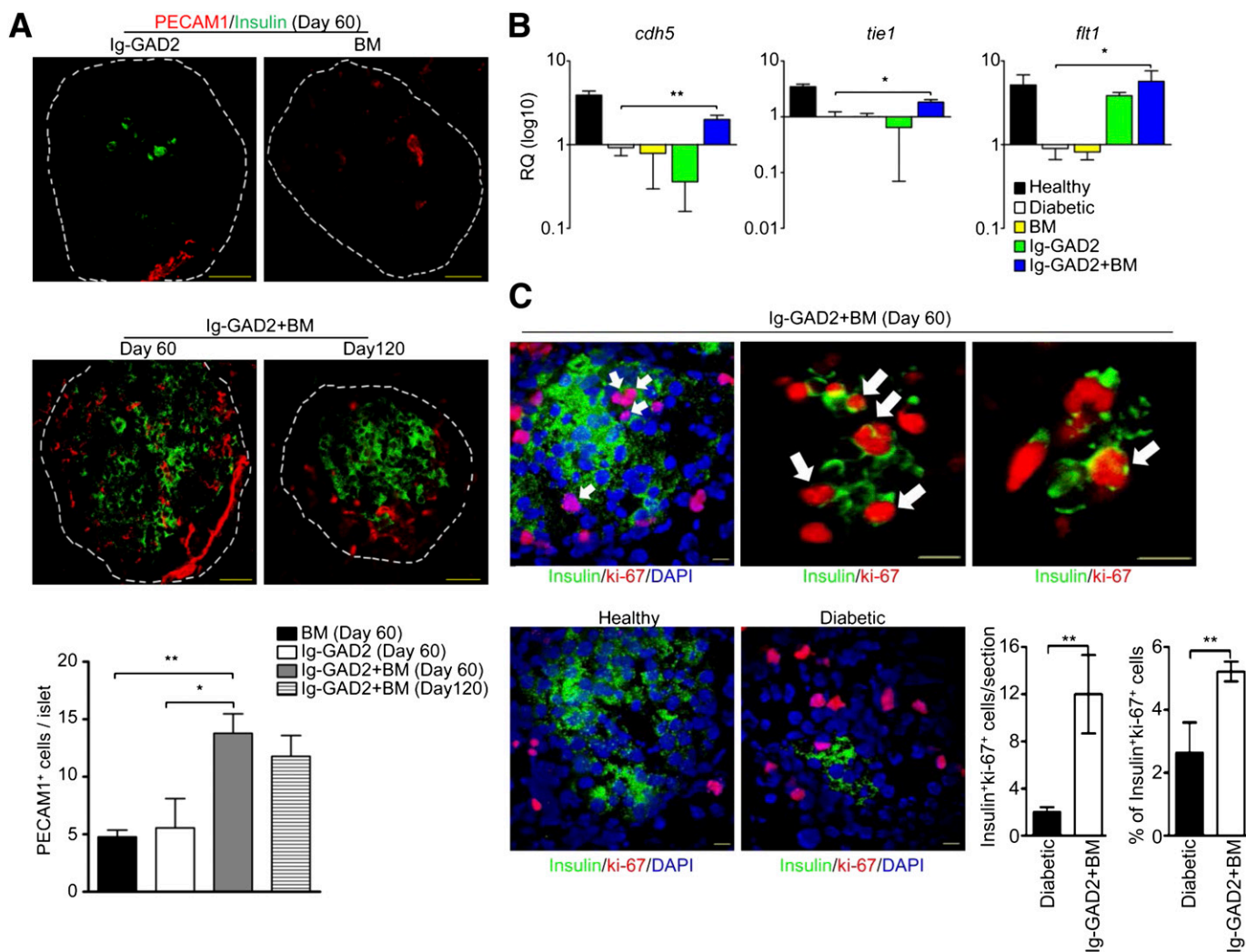
FIG. 5. Restoration of ECs parallels with β-cell regeneration. *A*: Fluorescence microscopy images of PECAM1 (red) and insulin (green) immunostaining of pancreatic sections from mice given Ig-GAD2, BM, or Ig-GAD2+BM. Islet boundary is depicted by dashed lines. Scale bars, 50 μm. The bar graph represents quantification of PECAM1+ cells per islet (five mice per group). Islets (10–30) from three to six nonserial sections per mouse were examined. *B*: Quantitative PCR analysis for *cdh5*, *tie1*, and *flt1* expression in pancreatic islets of the mice described in *A* as well as untreated healthy and diabetic controls (four to eight mice per group). *C*: Confocal microscopy images of insulin (green) and ki-67 (red) staining of pancreatic sections from Ig-GAD2+BM–treated (day 60 of treatment), healthy (untreated, 4–6 weeks of age), and diabetic (day 1 of diagnosis) mice. The arrows depict insulin+ki-67+ cells. Scale bars, 10 μm. The bar graphs represent the number of insulin+ki-67+ cells per section (*left*) and the ratio of insulin+ki-67+ over total insulin+ cells per pancreas (*right*). A total of 3,000 and 7,000 insulin+ cells were counted from 30–40 nonserial sections for the diabetic and Ig-GAD2+BM mice (six per group), respectively. The bars in the panels represent the mean ± SEM. *$P < 0.05$; **$P < 0.01$.

Fig. 3*B*), which is critical for the development of ECs and islet vascularization (29,30). The symbiotic relationship among ECs and β-cells is further evidenced by the parallel restoration of β-cell division in the Ig-GAD2+BM cell transfer mice (Fig. 5*C*). Indeed, the β-cells displayed significant staining for the proliferation marker ki-67 when compared with resting β-cells in normal mice or with residual β-cells in untreated diabetic mice (Fig. 5*C*). Indeed, the absolute cell number of ki-67+insulin+ cells was significantly higher in the Ig-GAD2+BM–treated versus control new-onset diabetic mice (Fig. 5*C*). This is further supported by a similar increase in the ratio of ki-67+insulin+ over total insulin+ cells (Fig. 5*C*). These results suggest that BM transfer during treatment with Ig-GAD2 sustained repair of the endothelial network leading to efficient regeneration of β-cells, which were able to produce the vital angiogenic factor VEGFa to maintain symbiosis and the health of the islets.

Donor BM transfer gives rise to islet ECs. To test whether the engrafted donor BM–derived GFP+ cells represent ECs, we examined the GFP+ cells for expression of the endothelial marker PECAM1 and for localization relative to insulin-producing β-cells. The results show that in the diabetes-free mice, there were GFP+ cells in the islets that expressed PECAM1, as indicated by the colocalization of the two markers at both day 30 and 60 of treatment (Fig. 6*A*). Such colocalization was not observed in mice receiving the same regimen that remained diabetic. Also, the GFP+PECAM1+ cells did not colocalize with insulin staining, indicating that the BM transfer gives rise to ECs during protection against T1D. These observations are supported by the detection of Y chromosome in the ECs but not in β-cells when the BM transfer was from male donors. Indeed, Y chromosome was detectable when the DNA was extracted from bulk pancreatic cells in mice receiving Ig-GAD2+BM (Fig. 6*B*). More specifically, when PECAM1+
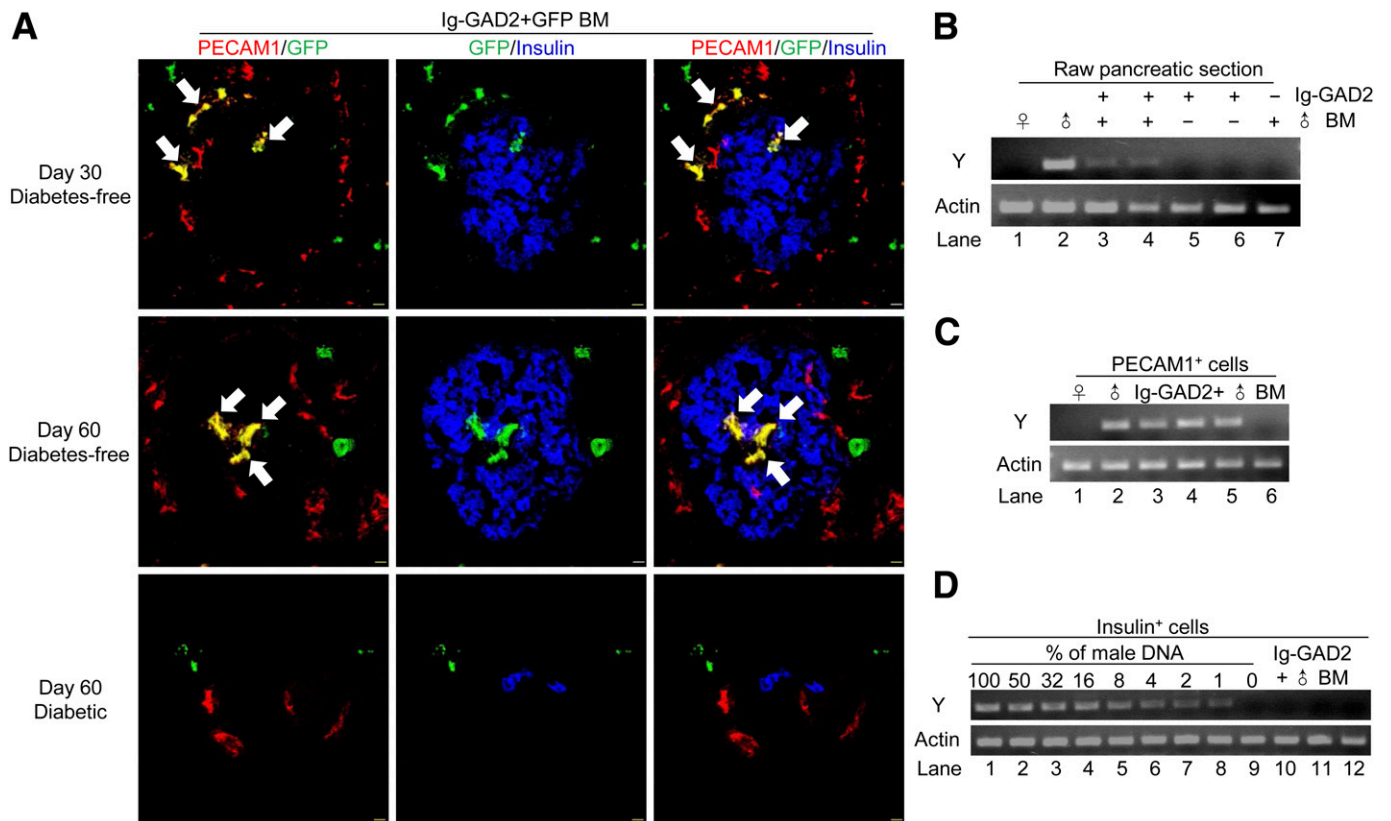
FIG. 6. Donor BM gives rise to pancreatic ECs during suppression of diabetes. *A*: Confocal microscopy images for insulin (blue), PECAM1 (red), and GFP (green) from mice given Ig-GAD2+NOD.GFP BM (five mice per time point). The arrows indicate colocalization of PECAM1 and GFP. Scale bars, 10 μm. *B–D*: PCR analysis of Y chromosome (Y) using genomic DNA extracted from raw pancreatic sections (*B*), microdissected PECAM1$^+$ (*C*), or insulin$^+$ cells (*D*) of mice given Ig-GAD2+male BM (killed on day 60 posttreatment). DNA extracted from unmanipulated male (♂) and female (♀) mice was included for control purposes. *C*: Lane 6 represents DNA from an Ig-GAD2+male BM–treated mouse that did not recover from diabetes. *D*: Lanes 1–9 represent the percentage of male DNA diluted with female DNA. Lanes 10–12 represent DNA from three individual diabetes-free mice given Ig-GAD2+male BM.

and insulin$^+$ cells were microdissected using a laser-capture system (Supplementary Fig. 4) and their genomic DNA was analyzed by PCR, Y chromosome was detected in PECAM1$^+$ but not insulin$^+$ cells, and this was restricted to diabetes-free mice given Ig-GAD2+BM transfer (Fig. 6C and D). These results indicate that donor BM gives rise to ECs that are required for recovery from diabetes.

EPCs substitute for BM transfer and assist Ig-GAD2 for reversal of T1D. EPCs are diminished in diabetic mice and human subjects (24–28). The transfer of BM alongside Ig-GAD2 treatment gave rise to pancreatic ECs (Fig. 6). These observations suggest that BM transfer during treatment with Ig-GAD2 likely provides EPCs that give rise to the increased frequency of mature ECs. If this were the case, transfer of donor EPCs instead of whole BM alongside Ig-GAD2 should yield mature ECs able to assist β-cells to thrive and restore normoglycemia. To test this premise, we first determined the frequency of EPCs in our NOD colony and found that the BM lineage–negative (Lin$^-$) population expressing the EPC markers c-Kit (31) and FLK-1 (32,33) was significantly reduced in the diabetic versus age-matched healthy mice (Fig. 7A and B). We then sorted these EPCs from BM of healthy NOD.GFP mice and determined whether these cells can substitute for whole BM to reverse T1D. Indeed, when sorted GFP$^+$Lin$^-$c-Kit$^+$FLK-1$^+$ (hFLK-1$^+$) cells from healthy donors replaced whole BM transfer during treatment with Ig-GAD2, most of the mice recovered from the disease, whereas the control

group given Lin$^-$c-Kit$^+$FLK-1$^-$ (hFLK-1$^-$) cells had a much lower recovery rate despite receiving a 60-times higher cell number (Fig. 7C). In addition, no significant recovery from disease was observed when the hFLK-1$^+$ cells were transferred without Ig-GAD2 (Fig. 7C). It has previously been shown that EPCs from diabetic subjects display impaired ability to differentiate into functional ECs (24). Thus, it is understandable that the diabetic mice were unable to use endogenous EPCs and required a transfer of cells from a healthy donor to recover from T1D upon treatment with Ig-GAD2. In fact, when the FLK-1$^+$ cells were derived from sick NOD.GFP mice (sFLK-1$^+$), there was minimal recovery from the disease as compared with the group receiving Ig-GAD2+hFLK-1$^+$ (*P* = 0.003840, area under the ROC curve) (Fig. 7C). Furthermore, there was no evident GFP$^+$ cells in the islets of these mice, which explains the lack of increase in PECAM1$^+$ cells (compare *right* and *left* in Fig. 7D). In fact, similar results were observed in the mice that did not recover from diabetes under the Ig-GAD2+FLK-1$^-$ or FLK-1$^+$ cells without Ig-GAD2 (Fig. 7D). These results indicate that EPCs can substitute for BM transfer and give rise to mature ECs that help β-cells thrive and restore normoglycemia. Furthermore, maturation of the EPCs and increase in ECs occur only when EPCs originate from healthy donors, which explains the inability of diabetic mice to use their own EPCs for repair of the pancreatic endothelial network.
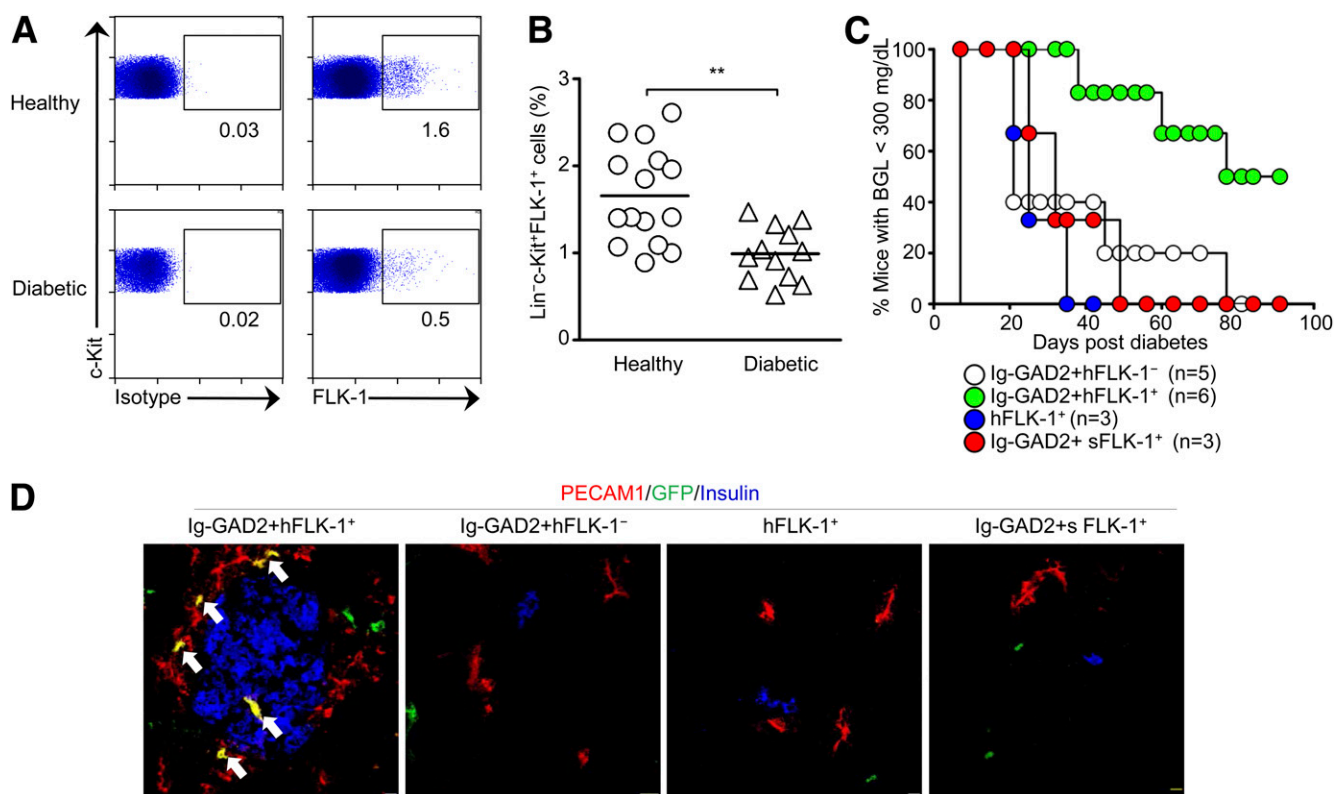
FIG. 7. Transfer of EPCs during treatment with Ig-GAD2 sustains β-cell regeneration and restores normoglycemia. *A*: Representative FACS plots depicting FLK-1 expression on Lin⁻c-Kit⁺7-AAD⁻ BM cells from age-matched healthy and diabetic mice. *B*: FLK-1 expression on Lin⁻c-Kit⁺7-AAD⁻ BM cells of individually tested mice described in *A*. *C* and *D*: FACS-sorted Lin⁻c-Kit⁺FLK-1⁺ (FLK-1⁺) or Lin⁻c-Kit⁺FLK-1⁻ (FLK-1⁻) BM cells from healthy (hFLK-1⁺) or diabetic (sFLK-1⁺) NOD.GFP donors were used with or without Ig-GAD2 for treatment of diabetic NOD mice. Some of the mice were monitored for diabetes for 100 days (*C*), and others (*D*) were killed on day 60 posttreatment and used for visualizing insulin (blue), PECAM1 (red), and GFP by confocal microscopy (at least 20 sections per group). The arrows indicate colocalization of PECAM1 and GFP. Scale bars, 10 μm. **P < 0.01.

DISCUSSION

Recent advances have shown that treatment with anti-CD3 antibody can reverse overt diabetes (34,35). However, because of potential interference with the function of the immune system, open-ended treatment regimens are undesirable (36). In this context, antigen-specific approaches (37–42) that target autoreactive T cells and circumvent interference with immunity provide an alternative that could be effective against the disease. We and others have tested cell or protein-based antigen-specific regimens at advanced stages of the disease, and promising outcomes were observed (7,43,44). In fact, Ig-GAD2 was able to trigger β-cell regeneration, which prevented progress to overt diabetes (7). The current study was designed to test Ig-GAD2 for efficacy against overt T1D. However, despite the induction of an immune modulation similar to the hyperglycemic stage, the regimen was not able to trigger β-cell regeneration or overcome overt T1D. Given that β-cells are able to self-renew (12), we thought that either the differentiation of stem cell progenitors into insulin-producing β-cells is defective at this stage of the disease or there were minimal residual β-cells to support division and formation of sufficient β-cell mass. Although the use of BM as a source of β-cell progenitors is debatable (8,9,16,17,45), repair of injured islet was feasible by BM transplantation (8,9). Thus, we supplemented Ig-GAD2 treatment with BM transfer and found that recovery from disease is attainable. This was intriguing and prompted us to determine the mechanism underlying protection against

disease. Interestingly, the islets had increased β-cell mass, but the proliferating insulin-producing cells were of endogenous origin rather than donor BM–derived cells. Surprisingly, alongside the newly formed β-cells, there was engraftment of donor BM–derived cells that did not produce insulin or colocalize with the β-cells.

It has previously been shown in human patients with recent onset of T1D that the number of EPCs is significantly reduced in the peripheral blood compared with sex-matched healthy control subjects (24,25). More importantly, EPCs in these patients displayed impaired migratory capacity (27) and damage repair potential (26), and failed to differentiate into functional vasculatures (24,25). Given that our NOD mice displayed diminished frequency of EPCs at the onset of diabetes, as was observed by others (25,28), we suspected that the engrafted donor BM–derived cells represent mature ECs. This was indeed the case, as the BM-derived GFP cells present in the islets of treated diabetes-free mice expressed the EC marker PECAM1. Moreover, PECAM1 expression tightly colocalized with donor GFP but not with newly formed endogenous β-cells. Since recovery from diabetes occurred only when the treatment was accompanied by BM transfer, it is likely that repair of the islet vascular system is required to maintain symbiosis among β-cells and ECs (18–23,29). This could explain the unexpected engraftment of donor BM–derived ECs in the pancreas of STZ mouse models of experimental diabetes (8,9), especially since the animals have undergone irradiation prior to BM

transplantation, which destroys endogenous stem cell precursors. Given that β-cells produced VEGFa and the angiogenic activity in the pancreas became evident, it is likely that repair of the islet vascular niche is required for β-cells to thrive and for insulin delivery into the circulation. Along this line of reasoning, we substituted whole BM with EPCs (Lin$^-$c-Kit$^+$FLK-1$^+$) during treatment with Ig-GAD2 and observed formation of donor-derived ECs alongside the generation of endogenous β-cells in the diabetes-free mice. Again, this suggests that under tight control of the immune inflammatory process, the symbiotic relationship between β-cells and ECs ensues and both types of cells contribute to the makeup of an environment suitable for formation of β-cells, maturation of ECs, and maintenance of healthy islets. Studies with anti-CD3 antibody indicated that despite control of the inflammatory process, β-cell proliferation/regeneration was minimal or at a very slow rate (15,46,47), with evident regranulation of residual insulin$^-$ β-cells (15). However, when eradication of inflammation was accompanied by exogenous epidermal growth factor, β-cell neogenesis and proliferation ensued and sustained reversal of overt T1D (48). The findings in our study suggest that the low frequency of EPCs and the defective function of the residual pancreatic endothelial network in patients with diabetes compromise not only the generation of new β-cells but also the restoration of optimal function, hence, the return of disease observed in human trials upon termination of anti-CD3 antibody treatment (4,5). In summary, antigen-specific therapy and supplementation with EPCs may overcome the limitation associated with long-term antibody administration and the repair of the islet endothelial niche. Whether effective control of immune inflammation by multiple Ig chimeras and diverse mechanisms (7,39,40,49,50) upon early diagnosis of disease would overcome the need for stem cell enrichment remains to be determined.

ACKNOWLEDGMENTS

REFERENCES

1. Atkinson MA, Eisenbarth GS. Type 1 diabetes: new perspectives on disease pathogenesis and treatment. Lancet 2001;358:221–229
2. Bluestone JA, Herold K, Eisenbarth G. Genetics, pathogenesis and clinical interventions in type 1 diabetes. Nature 2010;464:1293–1300
3. Belghith M, Bluestone JA, Barriot S, Mégret J, Bach JF, Chatenoud L. TGF-beta-dependent mechanisms mediate restoration of self-tolerance induced by antibodies to CD3 in overt autoimmune diabetes. Nat Med 2003;9:1202–1208
4. Herold KC, Hagopian W, Auger JA, et al. Anti-CD3 monoclonal antibody in new-onset type 1 diabetes mellitus. N Engl J Med 2002;346:1692–1698
5. Herold KC, Gitelman SE, Masharani U, et al. A single course of anti-CD3 monoclonal antibody hOKT3gamma1(Ala-Ala) results in improvement in C-peptide responses and clinical parameters for at least 2 years after onset of type 1 diabetes. Diabetes 2005;54:1763–1769
6. Kim SK, Tarbell KV, Sanna M, et al. Prevention of type I diabetes transfer by glutamic acid decarboxylase 65 peptide 206-220-specific T cells. Proc Natl Acad Sci USA 2004;101:14204–14209
7. Jain R, Tartar DM, Gregg RK, et al. Innocuous IFNgamma induced by adjuvant-free antigen restores normoglycemia in NOD mice through inhibition of IL-17 production. J Exp Med 2008;205:207–218
8. Hess D, Li L, Martin M, et al. Bone marrow-derived stem cells initiate pancreatic regeneration. Nat Biotechnol 2003;21:763–770
9. Mathews V, Hanson PT, Ford E, Fujita J, Polonsky KS, Graubert TA. Recruitment of bone marrow-derived endothelial cells to sites of pancreatic beta-cell injury. Diabetes 2004;53:91–98
10. Wallet MA, Flores RR, Wang Y, et al. MerTK regulates thymic selection of autoreactive T cells. Proc Natl Acad Sci USA 2009;106:4810–4815
11. Heit JJ, Apelqvist AA, Gu X, et al. Calcineurin/NFAT signalling regulates pancreatic beta-cell growth and function. Nature 2006;443:345–349
12. Dor Y, Brown J, Martinez OI, Melton DA. Adult pancreatic beta-cells are formed by self-duplication rather than stem-cell differentiation. Nature 2004;429:41–46
13. Koulmanda M, Budo E, Bonner-Weir S, et al. Modification of adverse inflammation is required to cure new-onset type 1 diabetic hosts. Proc Natl Acad Sci USA 2007;104:13074–13079
14. Koulmanda M, Bhasin M, Hoffman L, et al. Curative and beta cell regenerative effects of alpha1-antitrypsin treatment in autoimmune diabetic NOD mice. Proc Natl Acad Sci USA 2008;105:16242–16247
15. Ablamunits V, Sherry NA, Kushner JA, Herold KC. Autoimmunity and beta cell regeneration in mouse and human type 1 diabetes: the peace is not enough. Ann N Y Acad Sci 2007;1103:19–32
16. Choi JB, Uchino H, Azuma K, et al. Little evidence of transdifferentiation of bone marrow-derived cells into pancreatic beta cells. Diabetologia 2003; 46:1366–1374
17. Lechner A, Yang YG, Blacken RA, Wang L, Nolan AL, Habener JF. No evidence for significant transdifferentiation of bone marrow into pancreatic beta-cells in vivo. Diabetes 2004;53:616–623
18. Lammert E, Cleaver O, Melton D. Induction of pancreatic differentiation by signals from blood vessels. Science 2001;294:564–567
19. Cleaver O, Melton DA. Endothelial signaling during development. Nat Med 2003;9:661–668
20. Nikolova G, Jabs N, Konstantinova I, et al. The vascular basement membrane: a niche for insulin gene expression and Beta cell proliferation. Dev Cell 2006;10:397–405
21. Johansson M, Mattsson G, Andersson A, Jansson L, Carlsson PO. Islet endothelial cells and pancreatic beta-cell proliferation: studies in vitro and during pregnancy in adult rats. Endocrinology 2006;147:2315–2324
22. Kaido T, Yebra M, Cirulli V, Montgomery AM. Regulation of human beta-cell adhesion, motility, and insulin secretion by collagen IV and its receptor alpha1beta1. J Biol Chem 2004;279:53762–53769
23. Guney MA, Petersen CP, Boustani A, et al. Connective tissue growth factor acts within both endothelial cells and beta cells to promote proliferation of developing beta cells. Proc Natl Acad Sci USA 2011;108: 15242–15247
24. Loomans CJ, de Koning EJ, Staal FJ, et al. Endothelial progenitor cell dysfunction: a novel concept in the pathogenesis of vascular complications of type 1 diabetes. Diabetes 2004;53:195–199
25. Schatteman GC, Hanlon HD, Jiao C, Dodds SG, Christy BA. Blood-derived angioblasts accelerate blood-flow restoration in diabetic mice. J Clin Invest 2000;106:571–578
26. Caballero S, Sengupta N, Afzal A, et al. Ischemic vascular damage can be repaired by healthy, but not diabetic, endothelial progenitor cells. Diabetes 2007;56:960–967
27. Thum T, Fraccarollo D, Schultheiss M, et al. Endothelial nitric oxide synthase uncoupling impairs endothelial progenitor cell mobilization and function in diabetes. Diabetes 2007;56:666–674
28. Khoo CP, Valorani MG, Brittan M, et al. Characterization of endothelial progenitor cells in the NOD mouse as a source for cell therapies. Diabetes Metab Res Rev 2009;25:89–93
29. Brissova M, Shostak A, Shiota M, et al. Pancreatic islet production of vascular endothelial growth factor–a is essential for islet vascularization, revascularization, and function. Diabetes 2006;55:2974–2985
30. Lammert E, Gu G, McLaughlin M, et al. Role of VEGF-A in vascularization of pancreatic islets. Curr Biol 2003;13:1070–1074
31. Dentelli P, Rosso A, Balsamo A, et al. C-KIT, by interacting with the membrane-bound ligand, recruits endothelial progenitor cells to inflamed endothelium. Blood 2007;109:4264–4271

32. Peichev M, Naiyer AJ, Pereira D, et al. Expression of VEGFR-2 and AC133 by circulating human CD34(+) cells identifies a population of functional endothelial precursors. Blood 2000;95:952–958

33. Reyes M, Dudek A, Jahagirdar B, Koodie L, Marker PH, Verfaillie CM. Origin of endothelial progenitors in human postnatal bone marrow. J Clin Invest 2002;109:337–346

34. Chatenoud L, Bluestone JA. CD3-specific antibodies: a portal to the treatment of autoimmunity. Nat Rev Immunol 2007;7:622–632

35. Waldron-Lynch F, Herold KC. Immunomodulatory therapy to preserve pancreatic β-cell function in type 1 diabetes. Nat Rev Drug Discov 2011;10:439–452

36. Luo X, Herold KC, Miller SD. Immunotherapy of type 1 diabetes: where are we and where should we be going? Immunity 2010;32:488–499

37. Tian J, Clare-Salzler M, Herschenfeld A, et al. Modulating autoimmune responses to GAD inhibits disease progression and prolongs islet graft survival in diabetes-prone mice. Nat Med 1996;2:1348–1353

38. Tisch R, Liblau RS, Yang XD, Liblau P, McDevitt HO. Induction of GAD65-specific regulatory T-cells inhibits ongoing autoimmune diabetes in nonobese diabetic mice. Diabetes 1998;47:894–899

39. Gregg RK, Jain R, Schoenleber SJ, et al. A sudden decline in active membrane-bound TGF-beta impairs both T regulatory cell function and protection against autoimmune diabetes. J Immunol 2004;173:7308–7316

40. Gregg RK, Bell JJ, Lee HH, et al. IL-10 diminishes CTLA-4 expression on islet-resident T cells and sustains their activation rather than tolerance. J Immunol 2005;174:662–670

41. Agardh CD, Cilio CM, Lethagen A, et al. Clinical evidence for the safety of GAD65 immunomodulation in adult-onset autoimmune diabetes. J Diabetes Complications 2005;19:238–246

42. Michels AW, von Herrath M. 2011 update: antigen-specific therapy in type 1 diabetes. Curr Opin Endocrinol Diabetes Obes 2011;18:235–240

43. Li L, Yi Z, Wang B, Tisch R. Suppression of ongoing T cell-mediated autoimmunity by peptide-MHC class II dimer vaccination. J Immunol 2009;183:4809–4816

44. Tang Q, Henriksen KJ, Bi M, et al. In vitro-expanded antigen-specific regulatory T cells suppress autoimmune diabetes. J Exp Med 2004;199:1455–1465

45. Ianus A, Holz GG, Theise ND, Hussain MA. In vivo derivation of glucose-competent pancreatic endocrine cells from bone marrow without evidence of cell fusion. J Clin Invest 2003;111:843–850

46. Phillips JM, O'Reilly L, Bland C, Foulis AK, Cooke A. Patients with chronic pancreatitis have islet progenitor cells in their ducts, but reversal of overt diabetes in NOD mice by anti-CD3 shows no evidence for islet regeneration. Diabetes 2007;56:634–640

47. Takiishi T, Korf H, Van Belle TL, et al. Reversal of autoimmune diabetes by restoration of antigen-specific tolerance using genetically modified Lactococcus lactis in mice. J Clin Invest 2012;122:1717–1725

48. Wang M, Racine JJ, Song X, et al. Mixed chimerism and growth factors augment beta cell regeneration and reverse late-stage type 1 diabetes. Sci Transl Med 2012;4:133ra59

49. Tartar DM, VanMorlan AM, Wan X, et al. FoxP3+RORgammat+ T helper intermediates display suppressive function against autoimmune diabetes. J Immunol 2010;184:3377–3385

50. Wan X, Guloglu FB, VanMorlan AM, et al. Mechanisms underlying antigen-specific tolerance of stable and convertible Th17 cells during suppression of autoimmune diabetes. Diabetes 2012;61:2054–2065